Electronic Supplementary Information

15-Crown-5-ether-based supramolecular hydrogel with selection ability for potassium cation *via* gelation and colour change

Yuta Chabatake,[a] Tomoki Tanigawa,[b] Yuto Hirayama,[b] Ryo Taniguchi,[a] Akitaka Ito,[c,d] Kiyonori Takahashi,[e] Shin-ichiro Noro,[f] Tomoyuki Akutagawa,[g] Takayoshi Nakamura,[e,h] Masayuki Izumi [a,b,i] and Rika Ochi [*a,b,i]

[a.] *Faculty of Science and Technology, Kochi University, 2-5-1, Akebono-cho, Kochi 780-8520, Japan. E-mail: ochi@kochi-u.ac.jp*

[b.] *Graduate School of Integrated Arts and Sciences, 2-5-1, Akebono-cho, Kochi 780-8520, Japan.*

[c.] *School of Engineering Science, Kochi University of Technology, Kami, Ko-chi 782-8502, Japan.*

[d.] *Research Center for Molecular Design, Kochi University of Technology, Kami, Kochi 782-8502, Japan.*

[e.] *Research Institute for Electronic Science (RIES), Hokkaido University, N20W10, Kita-ku, Sapporo 001-0020, Japan.*

[f.] *Faculty of Environmental Earth Science, Hokkaido University, Sapporo 060-0810, Japan.*

[g.] *Institute of Multidisciplinary Research for Advanced Materials (IMRAM), Tohoku University, 2-1-1 Katahira, Aoba-ku, Sendai 980-8577, Japan.*

[h.] *Department of Chemistry, Graduate School of Advanced Science and Engineering, Hiroshima University, 1-3-1, Kagamiyama, Higashi-hiroshima 739-8526, Japan.*

[i.] *Research and Education Faculty, Kochi University, 2-5-1, Akebono-cho, Kochi 780-8520, Japan.*

1. Materials and Methods

Generals

Chemical reagents were purchased from Tokyo Chemical Industry Co., Ltd., FUJIFILM Wako Pure Chemical Co., or Watanabe Chemical Industries, Ltd., and used without further purification. Thin layer chromatography (TLC) was performed on TLC silica gel $60F_{254}$ (Merck). Column chromatography was performed on silica gel 60N (Kanto Chemical Co., Inc., spherical neutral, 63–210 μm). ^{1}H NMR and ^{13}C NMR spectra in $CDCl_3$, CD_3OD, or DMSO-d_6 were recorded on a JEOL ECA500 spectrometer, and chemical shifts were determined by tetramethylsilane (TMS) or residual non-deuterated solvents as the internal reference. Multiplicities are abbreviated as follows: s = singlet, d = doublet, t = triplet, q = quartet, m = multiplet, dd = double doublet, and br = broad. LRMS (ESI-MS) analyses was carried out using a Bruker amaZon SL mass spectrometer. HRMS (ESI-MS) analyses was carried out using a Thermo Scientific Exactive spectrometer. FT-IR spectra were recorded on a JEOL FT/IR-4100 spectrometer using KBr pellets in the range of 4000 to 500 cm^{-1}, with a resolution of 4 cm^{-1}.

Preparation of solution of 1·H

1·H (typically, 1.0 mg) was suspended in 200 mM Tris–HCl buffer (pH 6.4–9.0) in a glass vial with a screw cap (Mighty vial, Maruemu, Japan). The suspensions were heated to form homogeneous solutions. Then, the hot solution was cooled to room temperature (ca. 23°C) and incubated for about 10 min.

Measurements of temperature-dependent absorption spectra of 1^- solution

A solution of $\mathbf{1}^-$ ([**1**·H] = 25 mM in 0.2 M Tris–HCl buffer (pH 8.0), 0.1 mL) was transferred into an assembled quartz cell (path length: 0.1 mm, GL Sciences Inc., cat. no. AB10-UV-0.1 with cell adaptor, GL Sciences Inc., cat. no. CAS-10-1). The absorption spectra were measured upon heating from 25 to 85°C using a Jasco V-650 spectrometer equipped with an ETCS-761 temperature controller.

DFT calculations for 1·H and 2·H

Theoretical calculations were performed by using Gaussian 16W (Revision A.03) software.[1] Ground-state geometries of an ion (deprotonated $\mathbf{1}^-$), deprotonated $\mathbf{2}^-$), K^+ or Na^+), water molecule or supramolecular complex were optimized under the B3LYP/6-

31G(d,p) level[2] as in water by using a conductor-like polarizable continuum model (CPCM). Frequency calculations for the optimized geometries by identical methodologies did not give any negative frequencies, irrespective of the ion. Gibbs energy changes for successive processes to give 1:1 (with two aqua ligands) and 1:2 complexes (ΔG_1 (e.g., $\mathbf{1}^- + K^+ + 2H_2O \rightleftarrows \mathbf{1}^-/K^+(OH_2)_2$) and ΔG_2 (e.g., $\mathbf{1}^-/K^+(OH_2)_2 + \mathbf{1}^- \rightleftarrows \mathbf{1}^-/K^+/\mathbf{1}^- + 2H_2O$), respectively) were determined from Gibbs energies of optimized geometries. Free energy changes for total 1:2 complexation (e.g., $2 \times \mathbf{1}^- + K^+ \rightleftarrows \mathbf{1}^-/K^+/\mathbf{1}^-$) ΔG_{tot} were calculated as $\Delta G_1 + \Delta G_2$.

Synthesis

Cl-AAC-C6-COOH was synthesized according to previously reported method.[3] 4'-Aminobenzo-15-crown-5 and 4'-aminobenzo-18-crown-6 were synthesized by catalytic reduction of 4'-nitrobenzo-15-crown-5 and 4'-nitrobenzo-18-crown-6 with Pd/C and hydrogen, respectively.

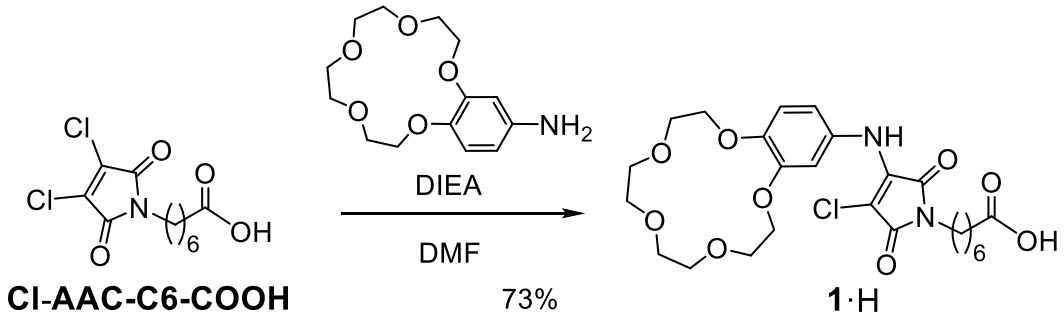

Cl-AAC-C6-COOH **1**·H

Scheme S1. Synthesis of **B15C5-AAC-C6-COOH** (**1**·H).

Synthesis of B15C5-AAC-C6-COOH (1·H): 4'-Aminobenzo-15-crown 5-ether (159 mg, 0.57 mmol, 1.1 eq.) and *N*, *N*-diisopropylethylamine (DIEA, 110 μL, 0.64 mmol, 1.25 eq.) were added to a solution of **Cl-AAC-C6-COOH** (150 mg, 0.51 mmol) in dry *N*, *N*-dimethylformamide (DMF, 10 mL), and the mixture was stirred at room temperature overnight under an N_2 atmosphere. The solvent was then evaporated, and the residue was purified by column chromatography (SiO_2, CH_2Cl_2:MeOH = 6:1 (*v*/*v*)). Then, the residue was further purified by reprecipitation with water and ethanol = 1/2 (*v*/*v*) for two times. The resulting product was dried under vacuum to give **1**·H (202 mg, 73%) as a yellow powder. ^{1}H NMR (500 MHz, CD_3OD): δ (ppm) = 1.29–1.42 (m, 4H), 1.58–1.64 (m, 4H),

2.27 (t, J = 7.5 Hz, 2H), 3.52 (t, J = 6.9 Hz, 2H), 3.71–3.74 (m, 8H), 3.87–3.88 (m, 4H), 4.12–4.15 (m, 4H), 6.77 (dd, J_1 = 2.3 Hz, J_2 = 8.6 Hz, 1H), 6.85 (d, J = 2.3 Hz, 1H), and 6.95 (d, J = 8.6 Hz, 1H). ^{13}C NMR (125 MHz, DMSO-d_6): δ (ppm) = 24.41, 25.89, 27.94, 28.09, 33.67, 37.69, 68.35, 68.70, 68.87, 69.72, 69.79, 70.46, 90.08, 110.81, 113.13, 116.64, 130.00, 138.40, 146.31, 147.84, 165.45, 167.43, 174.58. HRMS (ESI, positive mode): Calcd. for [M($C_{25}H_{33}ClN_2O_9$) + Na]$^+$: m/z = 563.1762; Found: 563.1767. FT-IR (KBr pellet): v = 3263.9, 3235.0, 2937.1, 2852.2, 1766.5, 1721.2, 1660.0, 1603.5, 1514.8, 1440.6, 1415.5, 1373.1, 1331.6, 1295.9, 1237.1, 1193.7, 1137.8, 1080.9, 1000.9, 981.6, 965.2, 939.2, 907.3, 874.6, 850.5, 937.4, 907.3, 874.6, 850.5, 797.4, 741.5, 650.9, 629.6, 525.5 cm^{-1}.

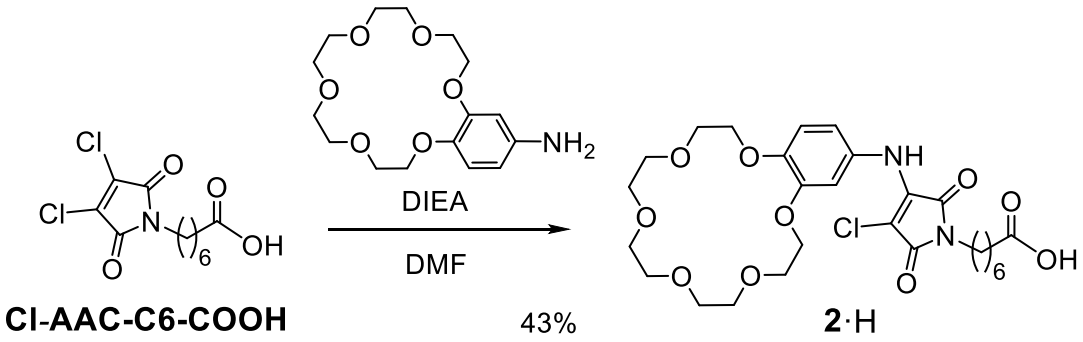

Scheme S2. Synthesis of **B18C6-AAC-C6-COOH** (**2**·H).

Synthesis of B18C6-AAC-C6-COOH (2·H): 4'-Aminobenzo-18-crown 6-ether (101 mg, 0.31 mmol, 1.0 eq.) and DIEA (53 μL, 0.31 mmol, 1.0 eq.) were added to a solution of **Cl-AAC-C6-COOH** (88 mg, 0.30 mmol) in dry DMF (3 mL), and the mixture was stirred at room temperature overnight under an N_2 atmosphere. The reaction mixture was dissolved in ethyl acetate (EtOAc, 150 mL), and the solution was washed with water (100 mL) for three times. The organic layer was collected, dried over anhydrous $MgSO_4$, and filtered. The filtrate was evaporated, and the residue was purified by column chromatography (SiO_2, CH_2Cl_2:MeOH = 6:1 to 3:1 (v/v)). Then, the residue was further purified by reprecipitation with hexane for five times. The resulting product was dried under vacuum to give **2**·H (76 mg, 43%) as an orange powder. ^{1}H NMR (500 MHz, CD_3OD): δ (ppm) = 1.29–1.41 (m, 4H), 1.58–1.64 (m, 4H), 2.29 (t, J = 7.5 Hz, 2H), 3.52 (t, J = 7.2 nh Hz, 2H), 3.65–3.66 (m, 4H), 3.68–3.69 (m, 4H), 3.72–3.74 (m, 4H), 3.87–3.88 (m, 4H), 4.14–4.17 (m, 4H), 6.76 (dd, J_1 = 2.0 Hz, J_2 = 8.3 Hz, 1H), 6.84 (d, J = 2.3

Hz, 1H), and 6.94 (d, J = 8.6 Hz, 1H). ^{13}C NMR (125 MHz, DMSO-d_6): δ (ppm) = 24.44, 25.94, 28.01, 28.13, 33.65, 37.73, 68.01, 68.23, 68.64, 68.76, 69.83, 69.91, 90.01, 110.22, 112.25, 116.43, 129.78, 138.46, 145,95, 147.38, 165.51, 167.51, 174.50. LRMS (ESI, positive mode): Calcd. for [M($C_{27}H_{37}ClN_2O_{10}$) + Na]$^+$: m/z = 607.2; Found: 607.2. FT-IR (KBr pellet): ν = 3293.8, 2936.1, 2935.1, 2859.9, 1777.1, 1715.4, 1662.3, 1596.8, 1510.0, 1368.2, 1330.6, 1291.1, 1234.2, 1193.7, 1130.1, 1083.8, 1051.0, 1022.1, 998.9, 948.8, 916.0, 888.1, 869.7, 844.7, 811.9, 793.6, 736.7, 655.7, 606.5, 523.6 cm^{-1}.

2. Effect of pH on the solubility of 1·H

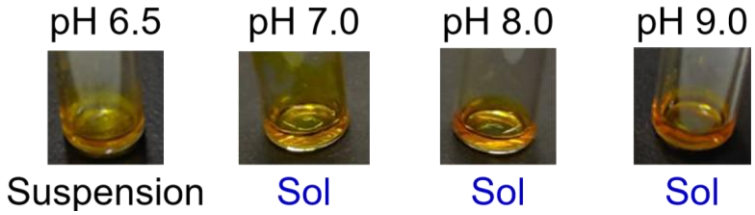

Figure S1. Photographs of **1**·H in 0.2 M Tris-HCl buffer (pH 6.4 to 9.0) after heated and allowed to cool to room temperature. Conditions: [**1**·H] = 25 mM in 0.2 M Tris-HCl buffer (pH 6.5 to 9.0).

3. Temperature-dependent absorption spectral change of the 1$^-$ solution

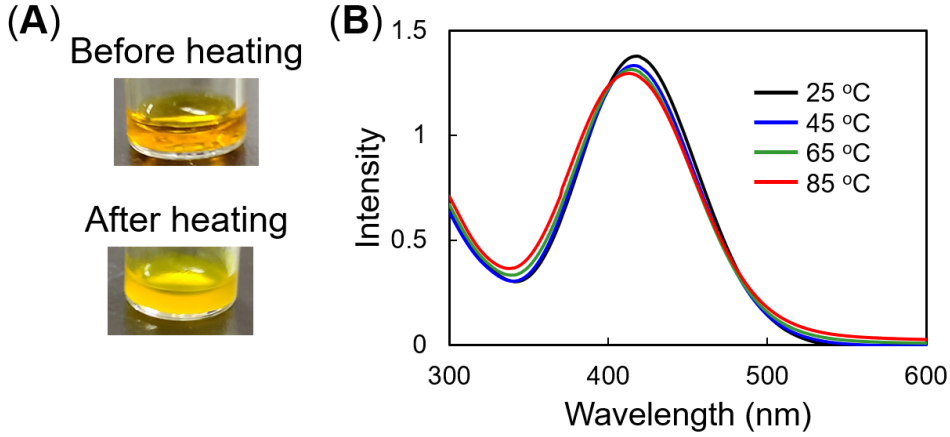

Figure S2. (**A**) Photograph of **1**$^-$ solution at room temperature (left) and after heating (right). (**B**) Absorption spectral changes of the solution **1**$^-$ upon heating. Conditions: [**1**·H] = 25 mM in 0.2 M Tris-HCl buffer (pH 8.0). Baseline rise at higher temperature was observed, which would be due to the increased sample turbidity. Furthermore, a blue shift of the maximum peak was observed with increasing temperature.

4. K^+ responsiveness of 1^- solution in the presence of Na^+

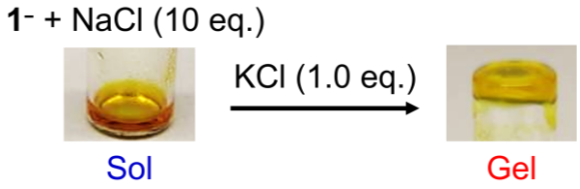

Figure S3. Photographs of $\mathbf{1}^-$ solution with NaCl aqueous solution (10 eq.) added (left) and the supramolecular hydrogel obtained by further addition of KCl (1.0 eq.) aqueous solution. Conditions: [**1**·H] = 25 mM, [NaCl] = 250 mM, [KCl] = 25 mM in 0.2 M Tris-HCl buffer (pH 8.0).

5. DFT Calculations for 1^-

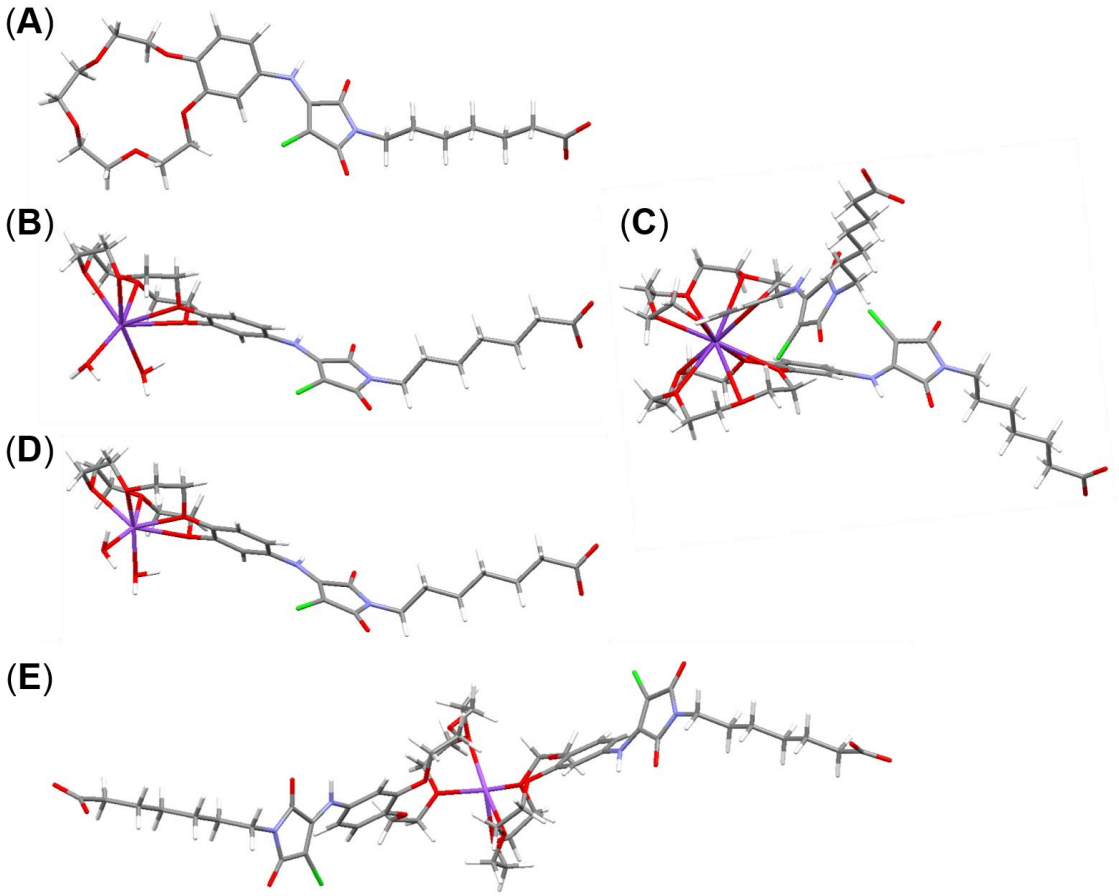

Figure S4. Optimized geometries of (A) $\mathbf{1}^-$, (B) $\mathbf{1}^-/K^+(OH_2)_3$, (C) $\mathbf{1}^-/K^+/\mathbf{1}^-$, (D) $\mathbf{1}^-/Na^+(OH_2)_2$ and (E) $\mathbf{1}^-/Na^+/\mathbf{1}^-$. Gray represent carbon, red: oxygen, light blue: nitrogen, light green: chlorine, white: hydrogen, and purple: potassium, light purple: sodium.

6. DFT Calculations for 2^-

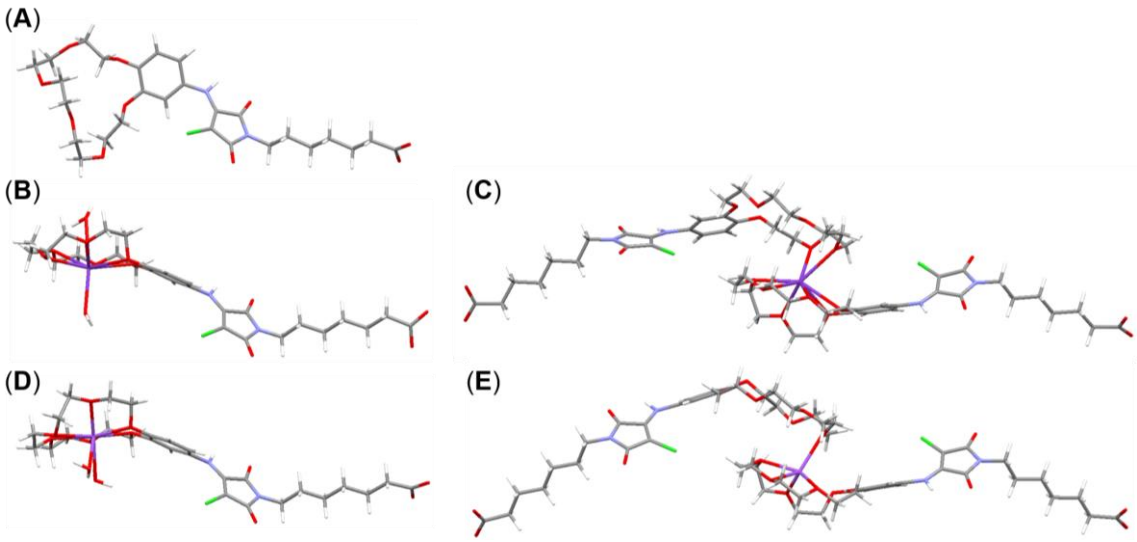

Figure S5. Optimized geometries of (A) $\mathbf{2}^-$, (B) $\mathbf{2}^-/K^+(OH_2)_2$, (C) $\mathbf{2}^-/K^+/\mathbf{2}^-$, (D) $\mathbf{2}^-/Na^+(OH_2)_2$ and (E) $\mathbf{2}^-/Na^+/\mathbf{2}^-$. Gray represent carbon, red: oxygen, light blue: nitrogen, light green: chlorine, white: hydrogen, and purple: potassium, light purple: sodium.

Table S1. Gibbs Energy Changes for Complexation Processes.

	$\mathbf{1}^-$	$\mathbf{2}^-$
K^+	$\Delta G_1 = -19.42$ kJ/mol	$\Delta G_1 = -50.94$ kJ/mol
	$\Delta G_2 = -22.21$ kJ/mol	$\Delta G_2 = -7.33$ kJ/mol
	$\Delta G_{tot} = -41.64$ kJ/mol	$\Delta G_{tot} = -58.27$ kJ/mol
Na^+	$\Delta G_1 = -36.65$ kJ/mol	$\Delta G_1 = -66.77$ kJ/mol
	$\Delta G_2 = +0.92$ kJ/mol	$\Delta G_2 = +15.51$ kJ/mol
	$\Delta G_{tot} = -35.73$ kJ/mol	$\Delta G_{tot} = -51.26$ kJ/mol

7. Rb^+ and Cs^+ responsiveness of 2^- solution

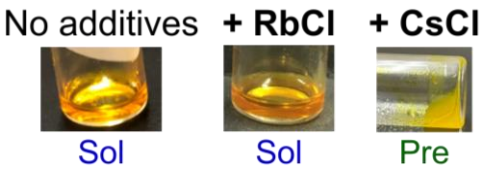

Figure S6. Photographs of the response of $\mathbf{2}^-$ to Rb^+ and Cs^+ (Sol: solution, Pre: precipitation). Conditions: [**2**·H] = 23 mM, [RbCl] = [CsCl] = 0 or 23 mM in 0.2 M Tris–HCl buffer (pH 8.0).

8. MS, ^{1}H NMR, ^{13}C NMR and IR spectra of 1·H and 2·H

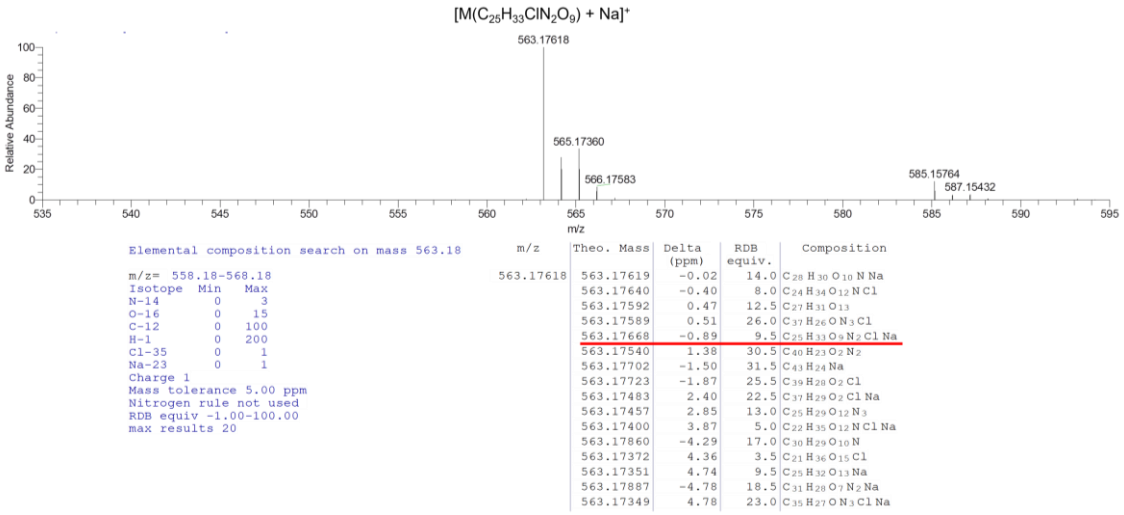

Figure S7. HRMS spectrum of **1**·H (ESI, positive mode).

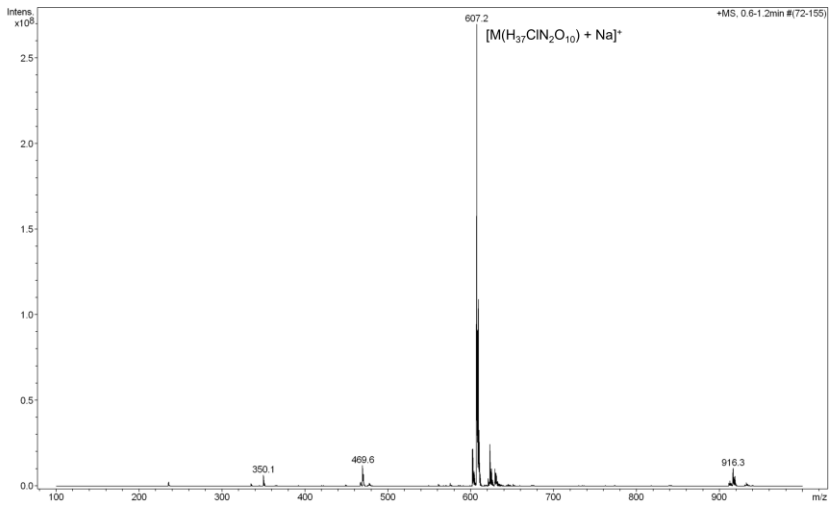

Figure S8. LRMS spectrum of **2**·H (ESI, positive mode).

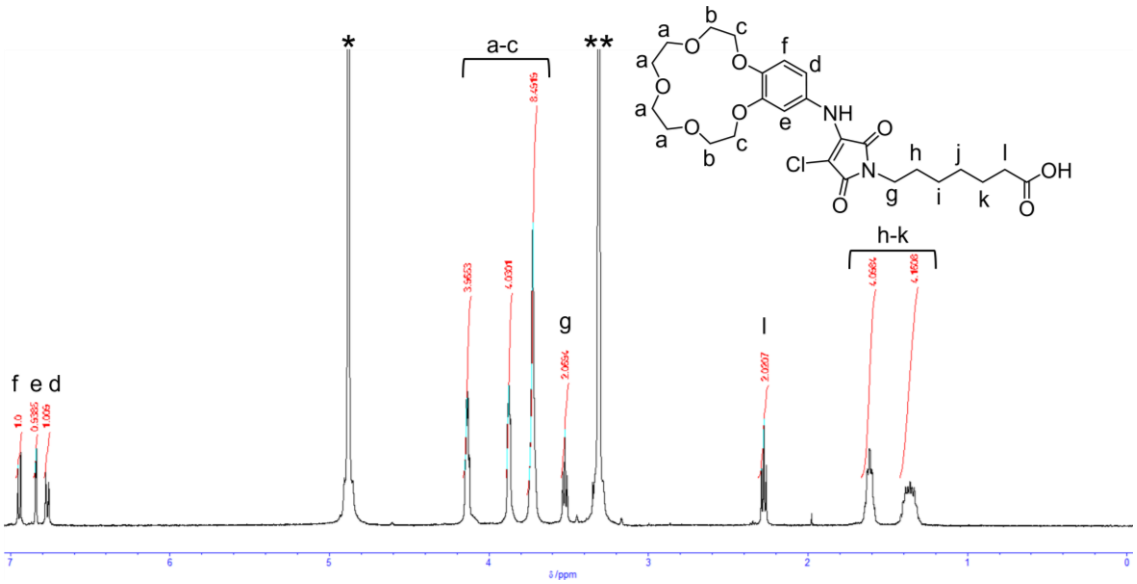

Figure S9. ^{1}H NMR spectrum (500 MHz, CD_3OD) of **1**·H. The peak labelled with an asterisk and double asterisk are attributed to water and residual non-deuterated solvent, respectively.

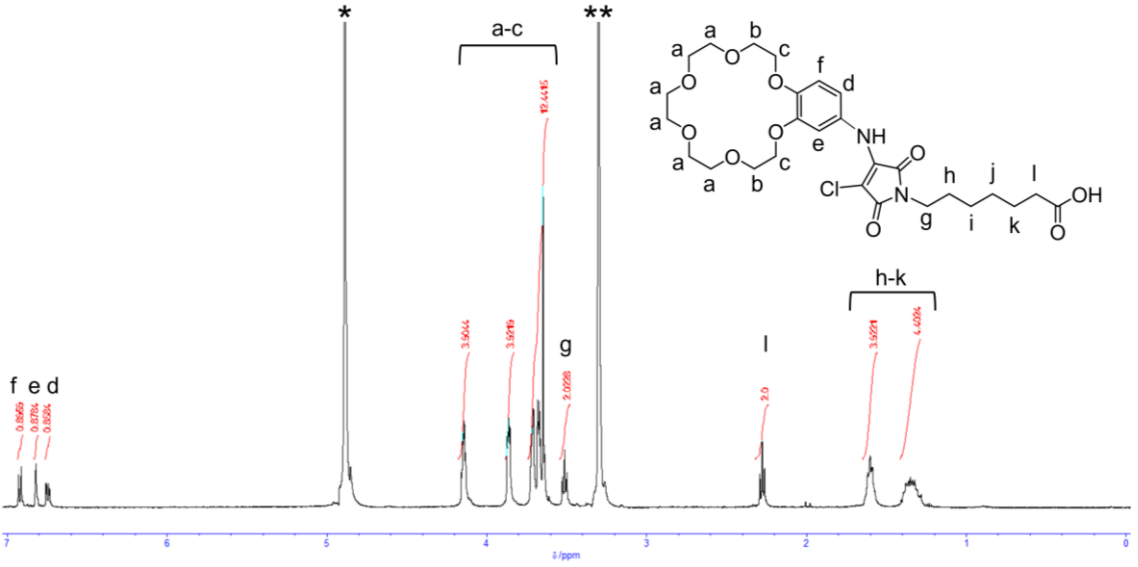

Figure S10. ^{1}H NMR spectrum (500 MHz, CD_3OD) of **2**·H. The peak labelled with an asterisk and double asterisk are attributed to water and residual non-deuterated solvent, respectively.

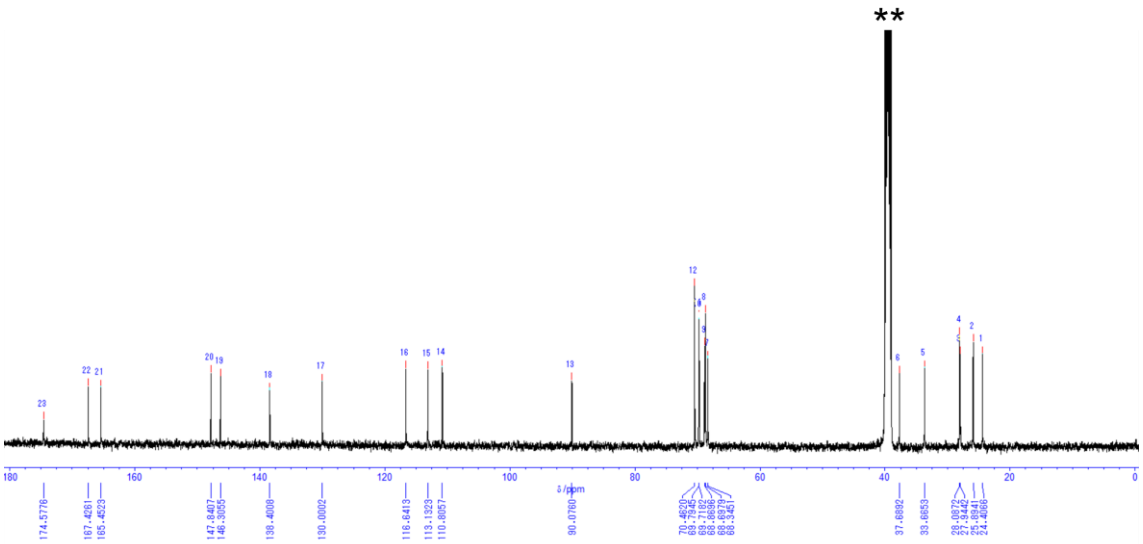

Figure S11. ^{13}C NMR spectrum (125 MHz, DMSO-d_6) of **1**·H. The peak labelled with double asterisk is attributed to residual non-deuterated solvent.

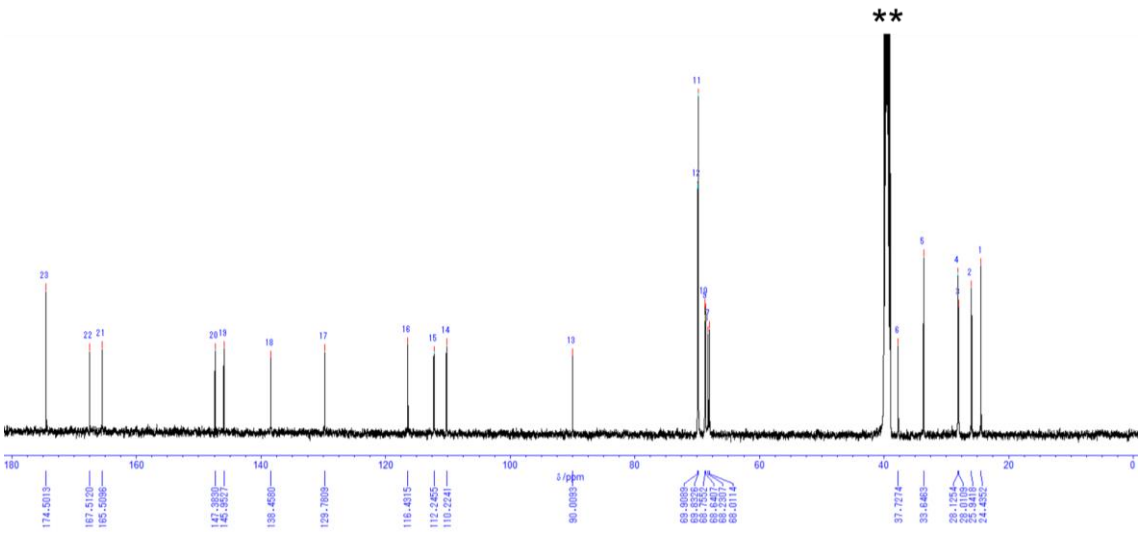

Figure S12. ^{13}C NMR spectrum (125 MHz, DMSO-d_6) of **2**·H. The peak labelled with double asterisk is attributed to residual non-deuterated solvent.

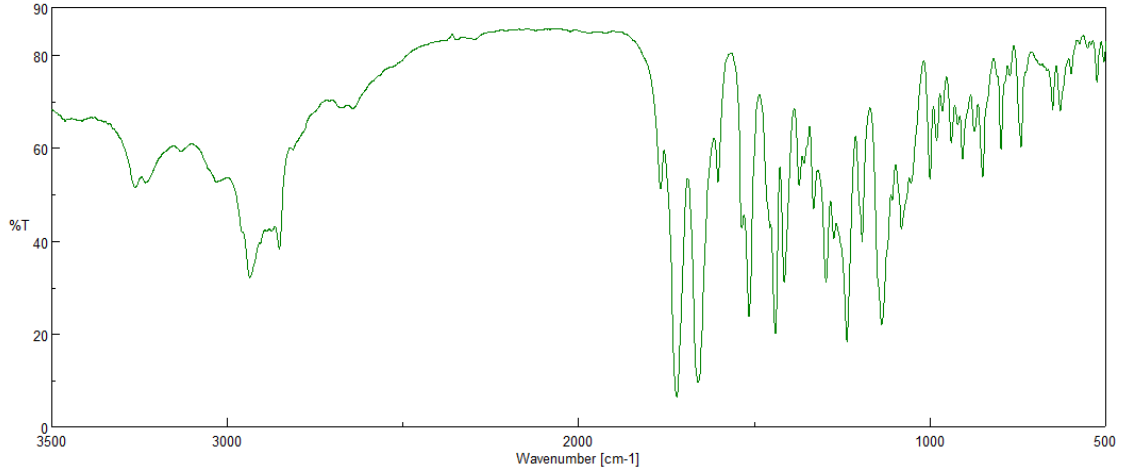

Figure S13. FT-IR spectrum of **1**·H (KBr pellet).

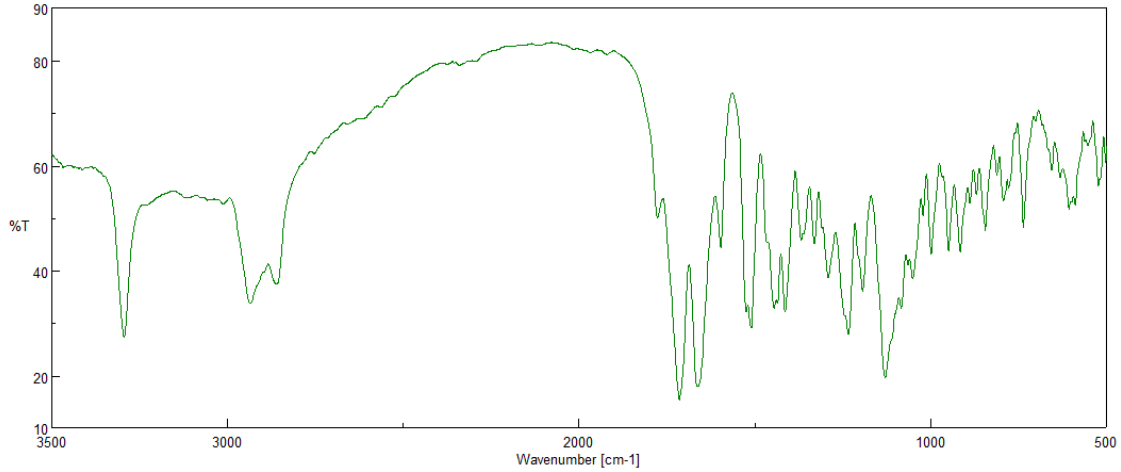

Figure S14. FT-IR spectrum of **2**·H (KBr pellet).

References

1. M. J. Frisch, G. W. Trucks, H. B. Schlegel, G. E. Scuseria, M. A. Robb, J. R. Cheeseman, G. Scalmani, V. Barone, G. A. Petersson, H. Nakatsuji, X. Li, M. Caricato, A. V. Marenich, J. Bloino, B. G. Janesko, R. Gomperts, B. Mennucci, H. P. Hratchian, J. V. Ortiz, A. F. Izmaylov, J. L. Sonnenberg, D. Williams-Young, F. Ding, F. Lipparini, F. Egidi, J. Goings, B. Peng, A. Petrone, T. Henderson, D. Ranasinghe, V. G. Zakrzewski, J. Gao, N. Rega, G. Zheng, W. Liang, M. Hada, M. Ehara, K. Toyota, R. Fukuda, J. Hasegawa, M. Ishida, T. Nakajima, Y. Honda, O. Kitao, H. Nakai, T. Vreven, K. Throssell, J. A. Montgomery Jr., J. E. Peralta, F. Ogliaro, M. J. Bearpark, J. J. Heyd, E. N. Brothers, K. N. Kudin, V. N. Staroverov, T. A. Keith, R. Kobayashi, J. Normand,

K. Raghavachari, A. P. Rendell, J. C. Burant, S. S. Iyengar, J. Tomasi, M. Cosso, J. M. Millam, M. Klene, C. Adamo, R. Cammi, J. W. Ochterski, R. L. Martin, K. Morokuma, O. Farkas, J. B. Foresman and D. J. Fox, Gaussian 16W (Revision A.03), Gaussian, Inc.: Wallingford CT, 2016.

2. G. A. Petersson and M. A. Al-Laham, *J. Chem. Phys.*, 1991, **94**, 6081.
3. R. Ochi, K. Kurotani, M. Ikeda, S. Kiyonaka and I. Hamachi, *Chem. Commun.*, 2013, **49**, 2115.